

Dual pH- and Temperature-Responsive Hydrogels with Extraordinary Swelling/Deswelling Behavior and Enhanced Mechanical Performances

Shutong Huang, Jianfeng Shen, Na Li, Mingxin Ye

Center of Special Materials and Technology, Fudan University, Shanghai 200433, China

Correspondence to: M. Ye (E-mail: mxye@fudan.edu.cn)

ABSTRACT: pH- and temperature-responsive semi-interpenetrating nanocomposite hydrogels (NC hydrogels) were prepared with surface-functionalized graphene oxide (GO) as the crosslinker, *N*-isopropylacrylamide (NIPAM) as the monomer, and chitosan (CS) as an additive. The effects of 3-(trimethoxysilyl)propylmethacrylate-modified GO sheets and CS content on various physical properties were investigated. Results show that PNIPAM/CS/GO hydrogels undergo a large volumetric change in response to temperature. Swelling ratios of PNIPAM/CS/GO hydrogels are much larger than those of the conventional organically crosslinked PNIPAM hydrogels. The deswelling test indicates that the deswelling rate was greatly enhanced by incorporating CS into the hydrogel network and using the surface-functionalized GO as the crosslinker. The pH-sensitivity of PNIPAM/CS/GO hydrogels is evident below their volume phase transition temperature. Moreover, the PNIPAM/CS/GO hydrogels have a much better mechanical property compared with traditional hydrogels even in a high water content of 90%. © 2014 Wiley Periodicals, Inc. *J. Appl. Polym. Sci.* **2015**, *132*, 41530.

KEYWORDS: biomaterials; hydrophilic polymers; mechanical properties; stimuli-sensitive polymers; swelling

Received 12 May 2014; accepted 14 September 2014

DOI: 10.1002/app.41530

INTRODUCTION

Hydrogels, which are three-dimensional polymer networks, are characterized by both hydrophilicity and insolubility in water and are capable of absorbing large amounts of water. In recent years, stimuli-sensitive hydrogel, a three-dimensional crosslinked polymer network, which is able to change its volume and properties in response to environmental stimuli such as temperature,¹ pH,² solvent composition,³ salt concentration,⁴ light,⁵ and magnetic field⁶ have attracted great interests. Among all the stimuli-sensitive hydrogels, a volume phase transition temperature (VPTT) of around 32°C makes poly(*N*-isopropylacrylamide) (PNIPAM) hydrogels particularly useful to prepare “smart” materials.^{7,8} Based on this phenomenon, a number of studies on PNIPAM and its copolymers were devoted to finding potential applications in various biomedical fields such as controlled drug delivery,^{9,10} chemical separation,^{11,12} enzyme immobilization,¹³ and artificial organ.¹⁴

A number of polysaccharides thus have been considered to be combined with the thermo-responsive PNIPAM to form smart hydrogels; and the one with the greatest potentiality is chitosan (CS), which is generally obtained from the deacetylation of chitin in a hot alkali solution. CS has been used in a variety of biomedical fields such as drug delivery carrier, surgical thread, and wound healing material.^{15,16} Furthermore, CS exhibits pH-responsive behavior due to the protonation–deprotonation equi-

librium of amino groups attached at the C2 position.^{17,18} Therefore, CS can be used as a hydrophilic polymer and a pH-responsive component to improve the swelling ratio of PNIPAM hydrogel and obtain pH-/temperature-responsive hydrogels.

Graphene, a very recent rising star in material science, with an atomically thin, 2D structure that consists of sp²-hybridized carbons, exhibits remarkable electronic,^{19–21} thermal,²² and mechanical properties.^{23,24} Due to plenty of hydrophilic oxygenated functional groups, graphene oxide (GO) can be easily exfoliated into monolayer sheets, which is stably dispersed in water.²⁵ The presence of oxygen-containing groups in graphene oxide renders it strongly hydrophilic and water-soluble, and also provides a handle for the chemical modification of graphene using known carbon surface chemistry. Therefore, GO is an important building block for synthesizing various functional materials.^{26,27}

Usually, the PNIPAM hydrogels are prepared by free-radical copolymerization of the monomer NIPAM and a chemical organic crosslinker such as *N,N'*-methylenebisacrylamide (BIS).²⁸ However, their slow response rate and poor mechanical properties greatly restrict their applications.²⁹ Enormous efforts have been made to develop a new material that could overcome these disadvantages. For example, clay and modified GO were used as the multifunctional crosslinker to prepared novel semi-interpenetrating nanocomposite hydrogels in our previous

Table I. The Feed Compositions of the Hydrogels

Sample	NIPAM (g)	CS (g)	GO (g)	BIS (g)
PNIPAM/CS5/GO2	1.000	0.050	0.020	0
PNIPAM/CS5/GO4	1.000	0.050	0.040	0
PNIPAM/CS5/GO6	1.000	0.050	0.060	0
PNIPAM/CS5/GO8	1.000	0.050	0.080	0
PNIPAM/CS5/GO10	1.000	0.050	0.100	0
PNIPAM/CS10/GO4	1.000	0.100	0.040	0
PNIPAM/CS20/GO4	1.000	0.200	0.040	0
PNIPAM/GO4	1.000	0	0.040	0
PNIPAM/CS	1.000	0.050	0	0.020
PNIPAM	1.000	0	0	0.020

reports, and the as-prepared hydrogels exhibited significantly large water uptake and enhanced mechanical properties compared with the conventional hydrogels.^{30,31} And more recently, a novel kind of double network hydrogel (DN hydrogel) based on PNIPAM and polyacrylic acid (PAA) using BIS as the crosslinker was prepared in our previous report.³² Despite the favorable mechanical strength of the hydrogels, however, the crosslinking conditions may adversely affect the activity of the entrapped bioactive molecules, due to the use of potentially harmful crosslinking agents. Han and Yan prepared supramolecular hydrogels of CS and GO, in which GO worked as the two-dimensional crosslinker due to its multifunctional groups on both sides, and the as-prepared hydrogels showed a self-healing performance.³³ Zhang et al. prepared GO-clay-PNIPAM hybrid hydrogels, which exhibited a high mechanical strength and extensibility.³⁴ However, few reports dealt with hydrogels with high mechanical properties at water content of more than 90% which are required in the field of biomimic and biotissue engineering. Furthermore, no study has been done to prepare PNIPAM/CS/GO pH- and temperature-responsive hydrogels with GO sheets as the crosslinker.

Therefore, we successfully prepared a novel kind of PNIPAM/CS/GO hydrogels based on PNIPAM and CS using surface-functionalized GO as an effective multifunctional crosslinker instead of using the conventional organic crosslinker. We found that the NIPAM/CS/GO hydrogels exhibited extraordinary swelling/deswelling behavior and enhanced mechanical properties.

EXPERIMENTAL

Materials

Natural graphite powder was bought from Qingdao Huatai lubricant sealing S&T Co. NIPAM (98%), 3-(trimethoxysilyl)propylmethacrylate (TMSPMA, 97%), CS (weight-average molecular weight = 100,000–300,000 and with a deacetylation of 80–95%), potassium permanganate (KMnO₄), sodium nitrate (NaNO₃), *N,N,N',N'*-tetramethylethylenediamine (TEMED), ammonium persulfate (APS), and BIS were purchased from Sigma-Aldrich.

Preparation and Modification of Graphene Oxide Sheets

GO was prepared from natural graphite powder by modified Hummers method.³⁵ The GO was obtained via a freeze drying

procedure. The purified GO (200 mg) was redispersed into deionized water (200 mL) and the mixture was sonicated for 1 h. Subsequently, TMSPMA (0.4 mL) was injected into the GO solution with mechanical stirring at 25°C. The surface silanization of GO sheets was allowed to proceed for 24 h. Surface modified GO sheets were then collected and washed with deionized water several times.

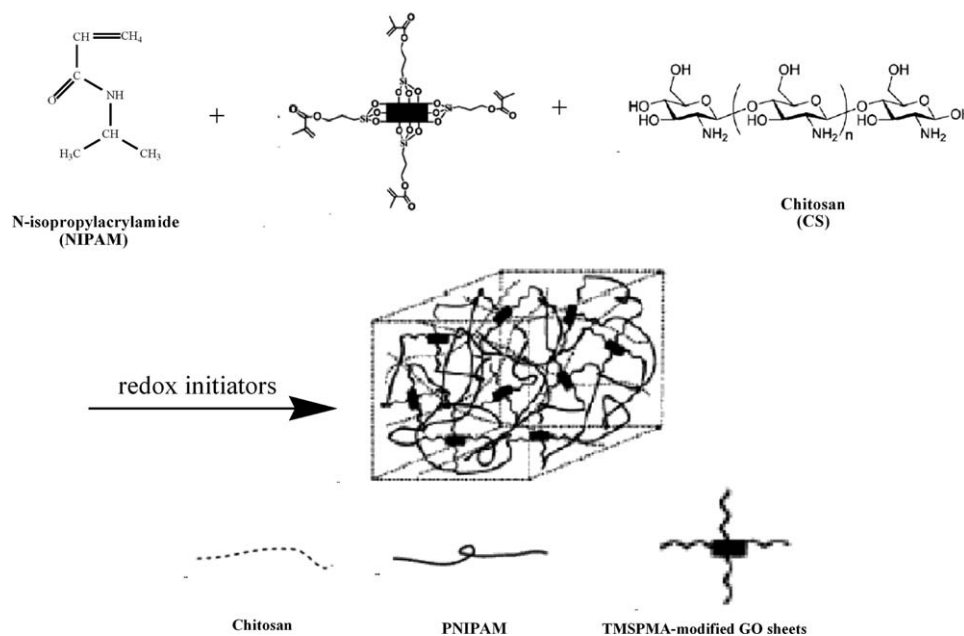
Preparation of PNIPAM/CS/GO Hydrogels

To prepare the PNIPAM/CS/GO hydrogels, the initial solution consisting of monomer NIPAM (1 g), deionized water (8.0 mL), and various ratios of GO sheets modified by TMSPMA was stirred in an ice-water bath for 2 h. Then the catalyst TEMED (20 μ L) and various ratios of CS (dissolved in 1.5 mL 0.2M acetic acid) were added with stirring. Finally, an aqueous solution of the initiator APS (0.02 g in H₂O 0.5 mL) was added into the solution. The free radical polymerization was carried out in a water bath at 20°C for 24 h. The hydrogels crosslinked by GO sheets are expressed as PNIPAM/CS m /GO n hydrogels. The number m and n represent the weight percent of CS and GO sheets relative to the NIPAM monomer, respectively. The conventional PNIPAM hydrogel crosslinked by BIS was also prepared for comparison. Three or more hydrogels were prepared for each sample formulation and analyzed in compressive test, water uptake, and deswelling experiments to obtain the standard deviation for each data point represented by error bars in the presented figures. The as-prepared hydrogels were purified by immersing into excess deionized water for 48 h with daily replacement of water to remove any water-soluble impurities. Then, the purified hydrogels were freeze dried before characterizations. The compositions of the PNIPAM/CS/GO hydrogels are shown in Table I.

Measurements

Fourier-transform infrared spectroscopy (FTIR) spectra were recorded on a NEXUS 670 spectrometer. X-ray diffraction (XRD) patterns were obtained with Cu-K α X-rays performed on a D/max- γ B X-ray diffractometer (40 kV, 30 mA) in a step of 0.02° s⁻¹ from 5° to 40°. Raman spectra of solid sample were obtained by use of a SPEX/403. The morphology of the freeze dried specimens was observed on a SUPERSCAN SSX-550 scanning electron microscope (SEM) at 20 kV after sputter coating with gold under vacuum. Several positions of the samples were imaged. The VPTT measurements of the wet samples were carried out on a TAQ100 differential scanning calorimeter (DSC) under a nitrogen atmosphere with a heating rate of 3°C min⁻¹ from 25 to 35°C. Thermogravimetric (TG) analyses were conducted with Netzsch TG 209F1, heating sample from ambient temperature to 700°C with a heating rate of 20°C min⁻¹ in a nitrogen atmosphere.

The mechanical properties of the cylindrical hydrogels were tested using a CMT 4204. For the compression tests, the hydrogel samples (column, with a diameter of 18 mm and height of 15 mm) with the same water content of 90% were placed between the self-leveling plates. Since the hydrogels are soft materials, all the samples were compressed at a rate of 3 mm min⁻¹ until the compression ratio reached 80%.



Scheme 1. The synthetic procedure of pH- and temperature-responsive hydrogels.

The swelling ratios of hydrogel samples were measured in the temperature range from 20 to 50°C or in a pH range from 1.2 to 9.0 by using a gravimetric method. The dried hydrogels were immersed in distilled water until their weight became constant. The hydrogels were then removed from the water and their surfaces were blotted with filter paper before being weighed. The swelling ratio was calculated with the following equation:

$$\text{Swelling ratio} = (W_s - W_d) / W_d, \quad (1)$$

where W_s is the weight of the swollen hydrogel and W_d is the weight of the dry hydrogel.

The deswelling behavior of the hydrogel was studied by recording the weight of water in the hydrogels. Water retention was calculated as

$$\text{Water retention} = (W_t - W_d) / (W_s - W_d), \quad (2)$$

where W_t is the weight of the hydrogel at a given time interval during the course of deswelling after the swollen hydrogel at 25°C had been quickly transferred into hot water at 45°C.

RESULTS AND DISCUSSION

Scheme 1 depicts the formation process of the PNIPAM/CS/GO hydrogels. The hydrogels were formed by *in situ* free-radical polymerization, in which the PNIPAM chains were crosslinked with multifunctional modified GO through covalent bond. The TMSMA-modified GO sheets are like chemical crosslinkers with multiple function groups, leading to the successful formation of hydrogels.

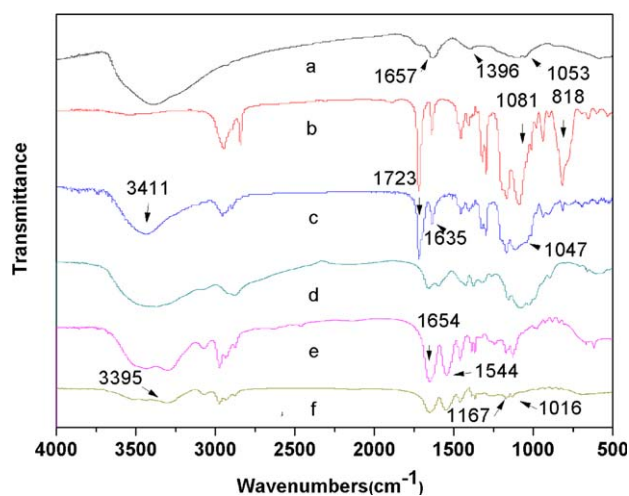


Figure 1. FTIR of (a) GO, (b) TMSMA, (c) TMSMA-modified GO sheets, (d) CS, (e) PNIPAM, and (f) the PNIPAM/CS/GO4 hydrogel. [Color figure can be viewed in the online issue, which is available at wileyonlinelibrary.com.]

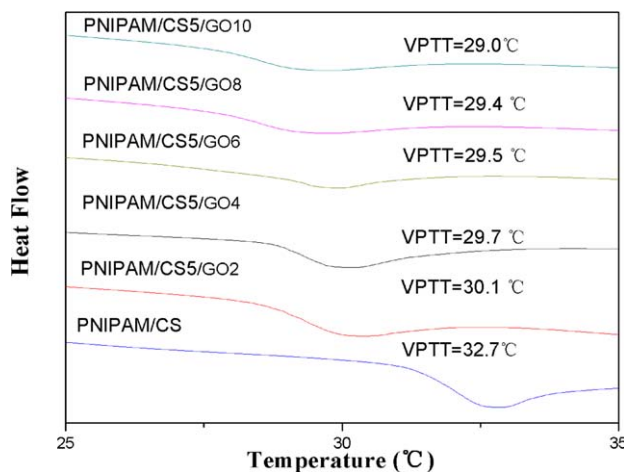


Figure 2. DSC thermograms of PNIPAM/CS and PNIPAM/CS/GO hydrogels. [Color figure can be viewed in the online issue, which is available at wileyonlinelibrary.com.]

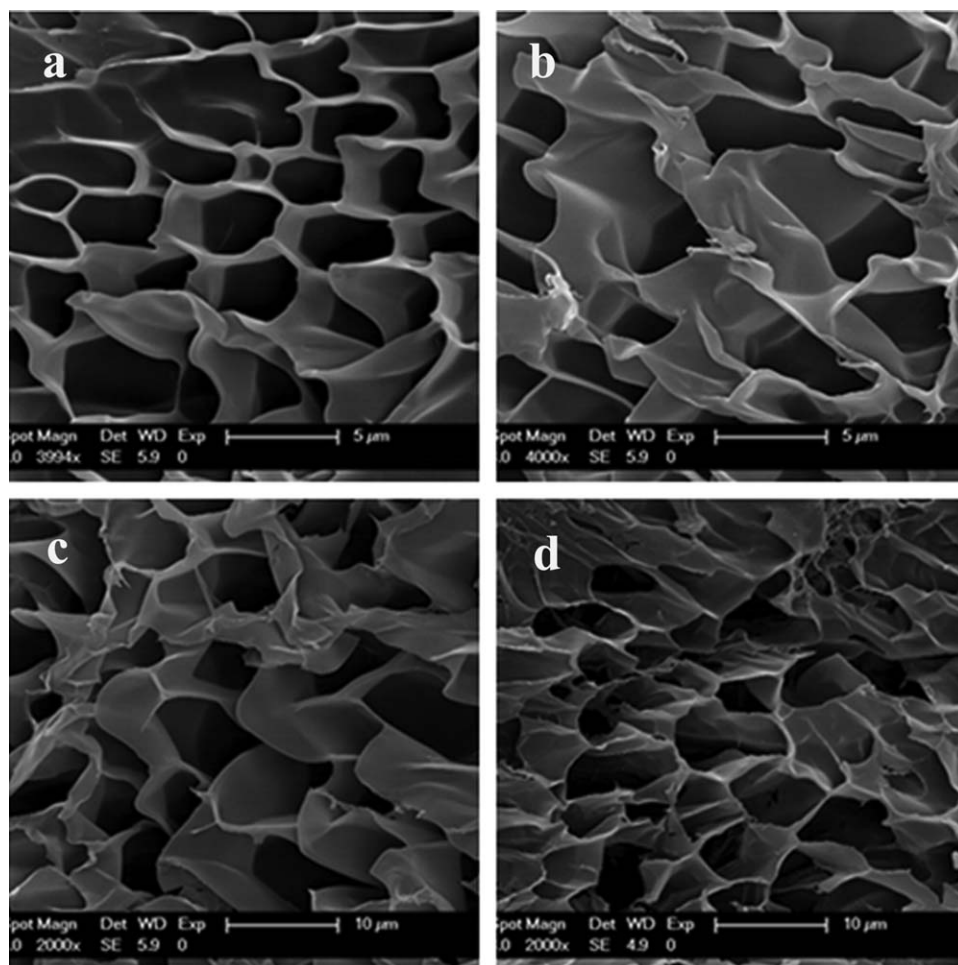


Figure 3. SEM images of freeze dried hydrogel of (a) PNIPAM, (b) PNIPAM/CS, (c) PNIPAM /CS5/GO2, and (d) PNIPAM/CS5/GO4.

FTIR Spectra Analysis

FTIR spectra of pure GO, pure TMSPMA, TMSPMA-modified GO sheets, CS, PNIPAM, and PNIPAM/CS5/GO4 hydrogel are shown in Figure 1. As shown in Figure 1, the characteristic vibrations of GO [Figure 1(a)] are the broad and intense peak of O—H groups centered at 3411 cm^{-1} , strong C=O peak at 1657 cm^{-1} , the O—H deformation peak at 1396 cm^{-1} , and the C—O stretching peak at 1053 cm^{-1} .³⁶ In the spectrum of TMSPMA-modified GO sheets [Figure 1(b)], there are many new peaks, most of which are the characteristic absorption peaks of TMSPMA. For instance, bands at 2955 cm^{-1} and 2893 cm^{-1} are linked to the stretching vibrations of $-\text{CH}_2$ groups, a strong band at 1723 cm^{-1} is ascribed to stretching vibration of the $-\text{CO}-$ groups and a band at 1047 cm^{-1} is related to the stretching vibration of Si—O groups. The band at 1635 cm^{-1} , which is related to the vinyl groups of the TMSPMA units on the sheets, demonstrates that the carbon-carbon double bonds ($\text{C}=\text{C}$) have been successfully introduced onto the surface of the GO sheets. The absorption peaks at 818 and 1081 cm^{-1} was not found, which indicates that the methoxysilyl groups ($\text{Si}-\text{O}-\text{CH}_3$) have been decomposed.³⁷ In conclusion, the FTIR results demonstrate that TMSPMA was

successfully grafted onto the GO sheets. From the spectrum of PNIPAM [Figure 1(e)], there is a stretching vibration (amide I) at 1654 cm^{-1} , N—H bending vibration (amide II) at 1544 cm^{-1} and two typical peaks of C—H vibrations of $-\text{CH}(\text{CH}_3)_2$. For the spectrum of PNIPAM/CS5/GO4 [Figure 1(f)], there are many new peaks, most of which are the characteristic absorption peaks of CS. For example, the peaks at 3395 cm^{-1} correspond to the N—H stretching vibration, and the absorption peaks at 1016 and 1167 cm^{-1} are attributed to the primary alcoholic group of C_6-OH and the secondary alcoholic group of C_3-OH . The peak at 1657 cm^{-1} is assigned to the carbonyl stretching vibration of the acetylated amino group.³³ This is solid evidence that chitosan can stably exist in the hydrogel network during the purification process. Therefore, it can be concluded that all the components used to form the semi-IPN hydrogels are present.

VPPT of the Hydrogels

The DSC thermograms of PNIPAM/CS and PNIPAM/CS/GO hydrogels are shown in Figure 2. The temperature at the onset point of the DSC endotherm is referred to the VPPT of the hydrogels.³⁸ At the VPPT, the water in the hydrogels will be

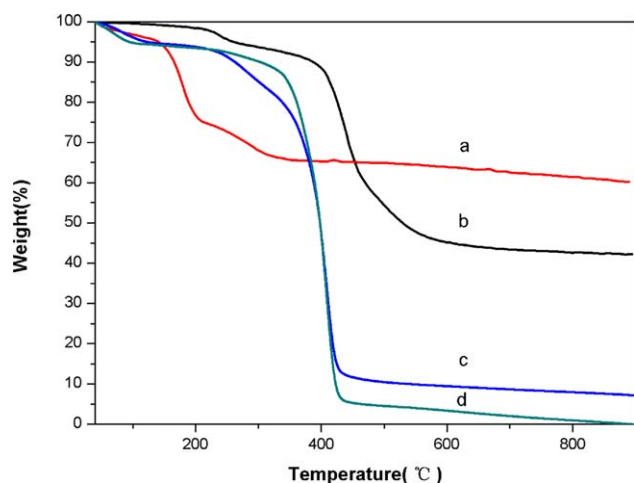


Figure 4. TGA curves of (a) GO sheets, (b) TMSPMA-modified GO sheets, (c) PNIPAM/CS5/GO4, and (d) PNIPAM/CS hydrogels. [Color figure can be viewed in the online issue, which is available at wileyonlinelibrary.com.]

separated from the network, which leads to a smaller heat capacity. As shown in Figure 2, while no significant deviation was observed from the VPTT of the PNIPAM hydrogel in the PNIPAM/CS, a significant deviation was observed when GO content is increased among the PNIPAM/CS/GO hydrogels. This is agreed with the findings of many literatures.^{30–32} This result indicates that while the introduction of CS into the PNIPAM network did not change the VPTT of the hydrogels, the incorporation of GO have a significant effect on the VPTT of the hydrogels. This may be explained that, on one hand, the interaction of the CS chain and the PNIPAM network gave a relatively independent polymer system, in which each retained its own properties, on the other hand the decrease of VPTT of the hydrogels is attributed to the hydrophilic–hydrophobic properties of the modified GO in the composite hydrogel. It is well known that PNIPAM hydrogels contain both hydrophilic $-\text{CONH}-$ and hydrophobic $-\text{CH}(\text{CH}_3)_2$ groups, and the temperature sensitivity of PNIPAM hydrogels arises from abrupt alterations in the hydrophilic/hydrophobic properties of these side groups at different temperatures.³⁹ Therefore, the VPTT of PNIPAM-based hydrogels is decreased by the incorporation of hydrophobic comonomers or increased with hydrophilic comonomers.^{40–44} The mechanism for the lower critical solution temperature (LCST) decrease here is similar to that of nanocomposite hydrogels reported previously, and is due to the hydrophobic nature of the incorporated materials (e.g., TMSPMA-modified GO).^{45,46} This decrease in the VPTT demonstrates the hydrophobic nature of the GO after modified by TMSPMA. Moreover, the outstanding thermal conduction of GO is beneficial to our temperature responsive hydrogel as faster heat conduction may facilitate faster response from the hydrogel. For example, an IR-light-responsive glycidyl methacrylate functionalized graphene-oxide (GO–GMA) incorporated hydrogel nanocomposite that undergoes significant volumetric change when irradiated by IR light has been reported by Lo.⁴⁷ In that report, it was fully illustrated that the superior thermal conductivity of GO can facilitate faster response from the hydrogel.

Morphological Studies

The morphological characteristics of hydrogels after exposure to solutions and subsequent freeze drying have been examined by SEM. Figure 3 shows the SEM images of the internal structure of PNIPAM [Figure 3(a)], PNIPAM/CS [Figure 3(b)], PNIPAM/CS5/GO2 [Figure 3(c)], and PNIPAM/CS5/GO4 [Figure 3(d)] hydrogels. Compared to PNIPAM hydrogel, PNIPAM/CS hydrogel exhibited the largest pore size ranging from 7 to 13 μm . In another word, a highly expanded network, which is beneficial to the swelling/shrinking process of hydrogel, can be generated by incorporating CS into the hydrogels network. This is critical to the swelling/shrinking process of hydrogels. Jin et al. have found that the swelling mechanism of the gels is determined by the microstructure related to the pore size and the thickness of struts.⁴⁸ Moreover, according to the SEM images, a natural conclusion can be easily drawn that the TMSPMA-modified GO sheets indeed behaved as a crosslinker. The TMSPMA-modified GO sheets are like chemical crosslinkers with multiple function groups, leading to the successful formation of hydrogels. Furthermore, it can be clearly seen that the PNIPAM/CS5/GO4 [Figure 3(c)] hydrogel appeared to have more compact porous structures compared with PNIPAM/CS5/GO2 [Figure 3(d)] hydrogel. It is because that the crosslinking density of the hydrogels increased with the increasing of GO content, resulting in the decrease in the pore size. As a result, the water molecules are hard to diffuse out when the temperature is above the hydrogel's VPTT. So, it can be concluded that the swelling ratio decreased with an increasing content of TMSPMA-modified GO sheets.

Thermogravimetric Analysis

The formation of surface-functionalized GO can also be confirmed by the TGA. As illustrated in Figure 4, GO was thermally unstable and more than 25% of its weight loss took place even below 200°C, which was due to the decomposition of the labile oxygen containing functional groups.⁴⁹ However, TMSPMA-modified GO, of which the labile groups had been removed via covalent attachment of GO with TMSPMA, was much more

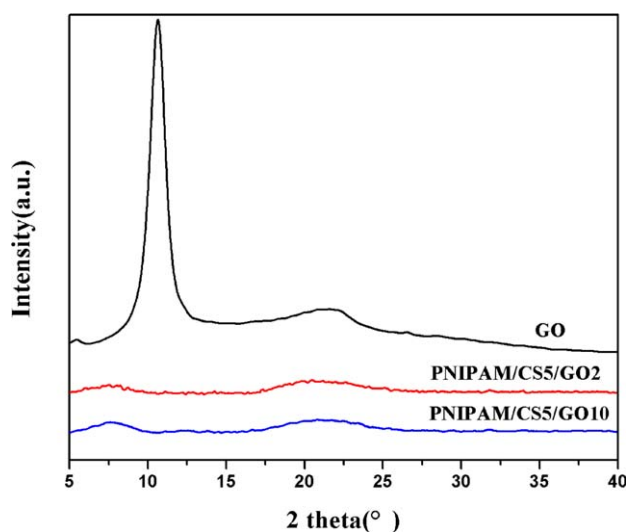


Figure 5. XRD patterns of (a) GO, (b) PNIPAM/CS5/GO2, and (c) PNIPAM/CS5/GO10 hydrogels. [Color figure can be viewed in the online issue, which is available at wileyonlinelibrary.com.]

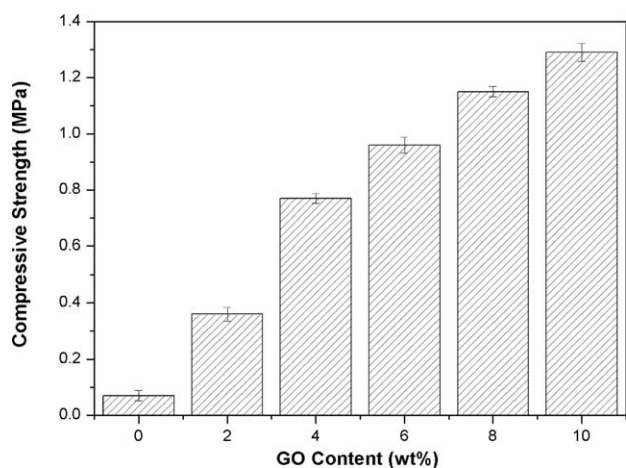


Figure 6. Compressive strength of PNIPAM/CS and PNIPAM/CS/GO hydrogels with different amounts of surface-functionalized GO.

thermally stable. It only showed less than 15% weight loss below 400°C. Then a major weight loss in the range from 400 to 550°C followed, as a result of decomposition of TMSPMA on the graphene sheet. Eventually, there was a very slow weight-loss process of TMSPMA-modified GO, from 550 to 900°C, which was assigned to the partial decomposition of the graphene sheets itself. Moreover, the amount of grafted TMSPMA was determined by TGA to be about 30 wt %, as shown in Figure 4. Compared to the feeding amount, only part of TMSPMA was successfully grafted onto the surface of the GO sheets. One thing to be noted here is that only the grafted TMSPMA could be preserved after purification. The C=C bonds of the grafted TMSPMA on the GO sheets can participate in the free radical polymerization. The PNIPAM/CS/GO hydrogels crosslinked with GO sheets were thus obtained. Moreover, it was observed that the PNIPAM/CS/GO hydrogels showed a higher thermal stability compared with the PNIPAM/CS hydrogel.

XRD Studies

As shown in Figure 5, it can be clearly seen that while almost no distinct diffraction peak at around for $2\theta = 11.2$ was

observed for the PNIPAM/CS5/GO2 [Figure 5(b)] and PNIPAM/CS5/GO10 [Figure 5(c)] hydrogels, the GO sheets [Figure 5(a)] showed a diffraction peak at $2\theta = 11.2$, corresponding to an interlayer spacing of 0.79 nm. Therefore, it can be concluded that GO sheets were uniformly dispersed in PNIPAM/CS/GO hydrogels.

Mechanical Properties

The compressive strength of PNIPAM/CS hydrogel and PNIPAM/CS5/GO hydrogels with different surface-functionalized GO content is shown in Figure 6. As shown in Figure 6, while the PNIPAM/CS hydrogel exhibits a poor compressive strength (only 0.07 MPa), the compressive strength of PNIPAM/CS5/GO hydrogels has been dramatically improved. For instance, the compressive strength of PNIPAM/CS5/GO6 hydrogel with 6 wt % of GO achieved at about 0.96 MPa, increased by about 1271% compared to the PNIPAM/CS hydrogel. Moreover, it was observed that the mechanical properties of PNIPAM/CS/GO hydrogels strongly depend on the contents of GO. The mechanical properties of PNIPAM/CS/GO hydrogels increased by increasing the contents of GO. This can be well explained by the large average inter-crosslinked distances in the PNIPAM/CS/GO hydrogel networks. The PNIPAM chains in the swollen state could be regarded as flexible polymer chains just like those in the rubbery state and thus the large deformation could be realized. Despite the high water content, the mechanical properties of the hydrogel were superior to many other reports. For instance, Fei et al. prepared a double-network (DN) hydrogels which achieved a compressive strength of 148 kPa,⁵⁰ which is far less than the strength of the PNIPAM/CS5/GO10 hydrogel with a water content of 90% in this study (Figure 6). It was fully illustrated by previous studies that the mechanical properties of the nanocomposite hydrogels became better with increasing GO content of the hydrogels.^{30,32} Through surface modification, GO can be well easily dispersed in water and can form a stable aqueous dispersion even with a high content of 10 wt %, therefore, we successfully increased the GO content in the PNIPAM hydrogels, as a consequence, the mechanical properties of these hydrogels were enhanced further.

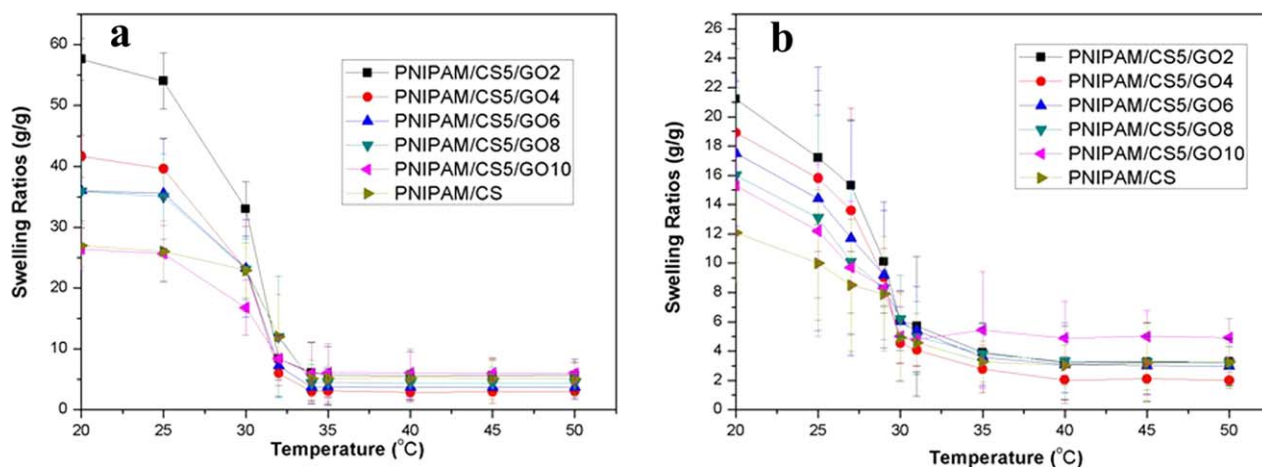


Figure 7. Swelling ratios of PNIPAM/CS/GO and PNIPAM/CS hydrogels as a function of temperature at pH 3.2 (a) and 9.2 (b). [Color figure can be viewed in the online issue, which is available at wileyonlinelibrary.com.]

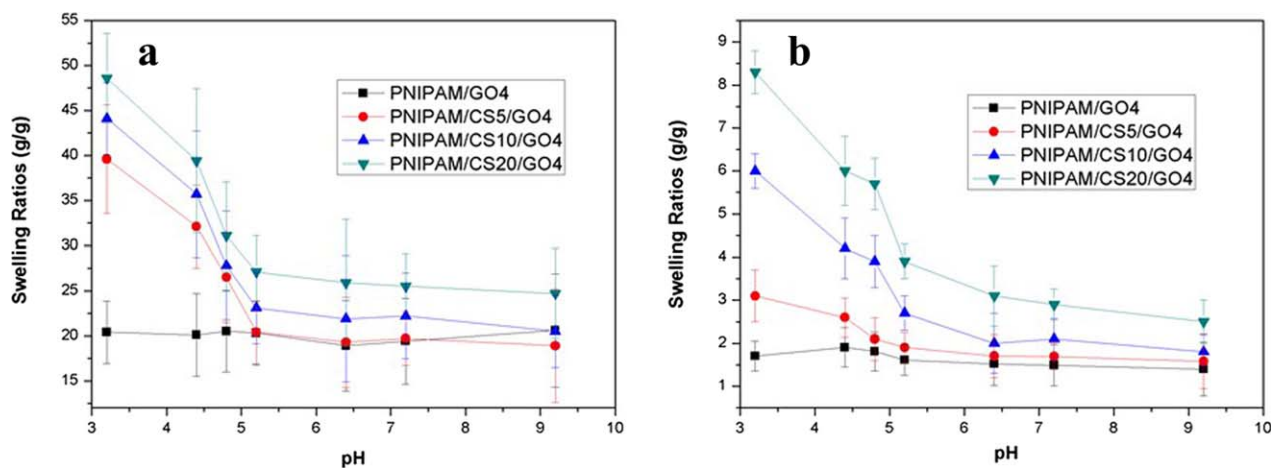


Figure 8. Swelling ratios of PNIPAM/CS/GO hydrogels as a function of pH at 25°C (a) and 35°C (b). [Color figure can be viewed in the online issue, which is available at wileyonlinelibrary.com.]

Temperature Dependence of the Hydrogels

The swelling ratios of PNIPAM/CS/GO hydrogels were investigated as a function of temperature at pH 3.2 [Figure 7(a)] and 9.2 [Figure 7(b)], as shown in Figure 7. It can be clearly seen that the introduction of GO sheets can dramatically increase the swelling ratio below VPTT. For example, in our previous report, the swelling ratio of PNIPAM/AA/GO DN hydrogels below VPTT is less than 25,³⁷ while for PNIPAM/CS/GO semi-IPN hydrogels, the swelling ratio is over 30, even reach 58 for the PNIPAM/CS5/GO2 at 20°C. In general, an abrupt decrease of the swelling ratios can be observed around VPTT for the samples, which is ascribed to the coil-globular transition of PNIPAM. The VPTT of the PNIPAM/CS/GO hydrogels are lowered by $\sim 3^\circ\text{C}$ and the volume collapses more gradually within a broader temperature range compared with the conventional PNIPAM hydrogel. The possible reason is that the incorporated TMSPMA-modified GO sheets within the networks produce a less dense hydrogel network than the conventional PNIPAM/CS hydrogel and thus there is extra volume in the precipitating water uptake. This interesting phenomenon may be due to many immobile water molecules interacting with the GO struc-

ture. Within the hydrogel networks, these GO sheets provide more interactions with water molecules, create more hydrogen bonding between water and hydrogel network, and the hydrogel thus holds more water molecules than traditional PNIPAM/CS hydrogels. Moreover, the swelling ratios of PNIPAM/CS/GO hydrogels gradually decreased by increasing the contents of GO. The PNIPAM/CS/GO hydrogels with higher GO contents led to more densely crosslinked networks, thus decreasing the swelling ratios of the hydrogels. At a basic pH [Figure 7(b)], the thermo-sensitivity of the hydrogels is similar to that in an acid pH. However, it can be seen in Figure 7 that the thermo-sensitivity of the hydrogels was weakened significantly at pH 9.2, and the VPTT of the hydrogel was decreased slightly. This is because, at high pH, the $-\text{NH}_2$ groups remain in the form $-\text{NH}_2$, which may induce the formation of inter- and intramolecular hydrogen bonding, so that hydrogen bonds become dominant in the polymer network resulting in a much more shrunken structure or a lower VPPT.⁵¹

pH Dependence of the Hydrogels

To investigate the influence of pH value of the medium on the swelling ratios for the PNIPAM/CS/GO hydrogels, the pH range is selected from 3.2 to 9.2 in this study. As shown in Figure 8, the swelling ratios of PNIPAM/CS/GO hydrogels gradually decreased with increasing pH of the buffer solution. This phenomenon may be attributed to the ionization behavior of the free amino groups in the chitosan derivative in response to external pH changes. Since the pK_a of the amino group of a glucosamine residue is about 6.5,⁵² most of the $-\text{NH}_2$ groups of chitosan chains are positively charged in acidic media, and electrostatic repulsion between the $-\text{NH}_3^+$ groups of chitosan chains causes the polymer network to expand. This attracts more water into the hydrogel network. In basic solution, the $-\text{NH}_2$ groups remain in the form $-\text{NH}_2$, which may induce the formation of inter- and intramolecular hydrogen bonding, so that hydrogen bonds become dominant in the polymer network. This enhancement of the interactions between polymer chains causes the observed decrease of the swelling ratio of the hydrogels. The result also revealed a dependence of the swelling ratio on the content of CS in the resulting hydrogels. The swelling ratio of

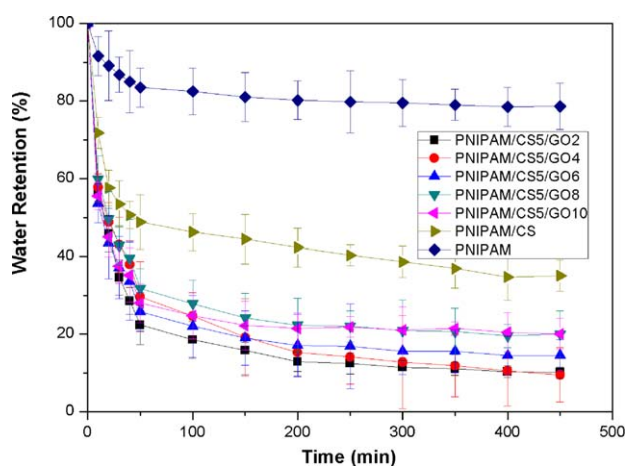


Figure 9. Deswelling behavior of conventional PNIPAM, PNIPAM/CS, and PNIPAM/CS/GO hydrogels at 45°C (pH 3.2). [Color figure can be viewed in the online issue, which is available at wileyonlinelibrary.com.]

the hydrogels increased with increasing the content of the chitosan at lower pH value, which may be attributed to the presence of more positively charged $-\text{NH}_2$ groups, which leads to an expansion in the hydrogel network. Moreover, while the PNIPAM/CS/GO hydrogels exhibited remarkable pH-sensitivity, as for the PNIPAM/GO hydrogel, the swelling ratios remain constant when pH changes in the range studied above. Since CS is the pH-responsive component, this is another proof of the stability of CS in the semi-IPN hydrogels in weak acid conditions. Compared with the remarkable pH-sensitivity of PNIPAM/CS/GO hydrogels in temperature below VPTT [Figure 8(a)], the pH-sensitivity of PNIPAM/CS/GO hydrogels in temperature above VPTT is not that obvious relatively [Figure 8(b)].

Deswelling Kinetics

As mentioned above, the deswelling rate is one of the most important factors and, in particular, high rates are needed in many applications. Figure 9 depicts the deswelling behaviors measured for hydrogels under the same experimental conditions. Contrary to pure PNIPAM hydrogel, the PNIPAM/CS/GO hydrogels exhibited rapid response. It is of interest to note that the deswelling curve of the PNIPAM/CS hydrogel is beneath that of the conventional PNIPAM hydrogel. In another word, the response rate was greatly enhanced by the incorporation CS into the hydrogels network during the deswelling process. These results indicated that a highly expanded network can be generated by electrostatic repulsions among $-\text{NH}_3^+$ groups of chitosan chains during the polymerization process. It is worthwhile to note that the PNIPAM/CS/GO hydrogels with low contents of GO have much higher response rates than the pure PNIPAM hydrogel. For instance, PNIPAM/CS5/GO2 hydrogel loses about 80% water within 2 h, whereas the conventional PNIPAM hydrogel takes 4 h to lose only 20% water. To describe the overall deswelling rate of the hydrogels, a reasonable criterion may be the time taken for the hydrogel to reach a half deswelling degree.⁵³ For the conventional PNIPAM/CS hydrogel, it requires about 50 min to attain the stable water retention of about 50%. However, the PNIPAM/CS5/GO2 hydrogel takes only about 10 min to reach the same deswelling degree. Furthermore, the deswelling rates gradually decreased as the contents of GO increased. However, a totally different result was observed in our previous report, in which the deswelling rates of the PNIPAM/AA/GO DN hydrogels increased with the increasing of the contents of GO and decreased with the increasing of the contents of AA.³² This is because GO was used as an additive in the PNIPAM/AA/GO DN hydrogels, while surface-functionalized GO was acted as crosslinker in the current work. By increasing GO content, therefore, the crosslink densities of the hydrogels increased, resulting in the decrease of the pore size. When the temperature is above the hydrogel's VPTT, the water molecules are difficult to diffuse out as a result of numerous small pores in the hydrogel network, thus the swelling ratio decreased by increasing the contents of GO. Moreover, while a highly expanded network can be generated by electrostatic repulsions among $-\text{NH}_3^+$ groups of chitosan chains in this experiment, higher acrylic acid content leading to more compact porous structures in the previous study, which is adverse to the diffusion of water molecules.

CONCLUSIONS

In this article, pH- and temperature-responsive PNIPAM/CS/GO hydrogels were prepared, which were crosslinked by GO sheets. TMPSMA-modified GO both acted as a multifunctional crosslinker and as reinforcing filler. The swelling ratios of hydrogels gradually decreased by increasing the contents of GO and increased by increasing the contents of CS. The pH sensitivity of PNIPAM/CS/GO hydrogels was evident below their VPTT. Also, the PNIPAM/CS/GO hydrogels exhibited high compressive strength even in high water content.

REFERENCES

1. Klier, J.; Scranton, A. B.; Peppas, N. A. *Macromolecules* **1990**, *23*, 4944.
2. Chiu, H.; Lin, Y.; Hung, S. *Macromolecules* **2002**, *35*, 5235.
3. Kokufata, E.; Zhang, Y. Q.; Tanaka, T. *Nature* **1991**, *351*, 302.
4. Dhara, D.; Chatterji, P. R. *Polymer* **2000**, *41*, 6133.
5. Suzuki, A.; Tanaka, T. *Nature* **1990**, *346*, 345.
6. Xulu, P. M.; Filipcsei, G.; Zrínyi, M. *Macromolecules* **2000**, *33*, 1716.
7. Tanaka, Y.; Kagami, Y.; Matsuda, A.; Osada, Y. *Macromolecules* **1995**, *28*, 2574.
8. Zhang, J.; Peppas, N. A. *J. Biomater. Sci. Polym. Edn.* **2002**, *13*, 511.
9. Tang, Y. F.; Zhao, Y. Y.; Li, Y.; Du, Y. M. *Polym. Bull.* **2010**, *64*, 791.
10. Hoffman, A. S. *Adv. Drug Deliv. Rev.* **2002**, *54*, 3.
11. Kawaguchi, H.; Fujimoto, K. *Bioseparation* **1998**, *7*, 253.
12. Zhang, Q. S.; Li, X. W.; Zhao, Y. P.; Chen, L. *Appl. Clay Sci.* **2009**, *46*, 346.
13. Liu, F.; Tao, G.; Zhuo, R. *Polym. J.* **1993**, *25*, 561.
14. Shiino, D.; Murata, Y.; Kataoka, K.; Koyama, Y.; Yokoyama, M.; Okano, T.; Sakurai, Y. *Biomaterials* **1994**, *15*, 121.
15. Dooley, T. P.; Ellis, A. L.; Belousova, M.; Petersen, D.; DeCarlo, A. A. *J. Biomater. Sci. Polym. Edn.* **2013**, *24*, 621.
16. Gu, Z.; Xie, H.; Huang, C.; Li, L.; Yu, X. *Int. J. Biol. Macromol.* **2013**, *58*, 121.
17. Denuziere, A.; Ferrier, D.; Domard, A. *Carbohydr. Polym.* **1996**, *29*, 317.
18. Lee, K. Y.; Park, W. H.; Ha, W. S. *J. Appl. Polym. Sci.* **1997**, *63*, 425.
19. Zhang, Y. B.; Tan, Y. W.; Stormer, H. L.; Kim, P. *Nature* **2005**, *438*, 201.
20. Rutter, G. M.; Crain, J. N.; Guisinger, N. P.; Li, T.; First, P. N.; Stroschio, J. A. *Science* **2007**, *317*, 219.
21. Oostinga, J. B.; Heersche, H. B.; Liu, X. L.; Morpurgo, A. F.; Vandersypen, L. *Nat. Mater.* **2008**, *7*, 151.
22. Balandin, A. A.; Ghosh, S.; Bao, W.; Calizo, I.; Teweldebrhan, D.; Miao, F.; Lau, C. N. *Nano Lett.* **2008**, *8*, 902.

23. Dikin, D. A.; Stankovich, S.; Zimney, E. J.; Piner, R. D.; Dommett, G. H. B.; Evmenenko, G.; Nguyen, S. T.; Ruoff, R. S. *Nature* **2007**, *448*, 457.
24. Park, S.; Lee, K.; Bozoklu, G.; Cai, W.; Nguyen, S. T.; Ruoff, R. S. *ACS Nano* **2008**, *2*, 572.
25. Cai, W. W.; Piner, R. D.; Stadermann, F. J.; Park, S.; Shaibat, M. A.; Ishii, Y.; Yang, D. X.; Velamakanni, A.; An, S. J.; Stoller, M.; An, J. H.; Chen, D. M.; Ruoff, R. S. *Science* **2008**, *321*, 1815.
26. Stankovich, S.; Dikin, D. A.; Dommett, G. H. B.; Kohlhaas, K. M.; Zimney, E. J.; Stach, E. A.; Piner, R. D.; Nguyen, S. T.; Ruoff, R. S. *Nature* **2006**, *442*, 282.
27. Su, Q.; Pang, S. P.; Alijani, V.; Li, C.; Feng, X. L.; Mullen, K. *Adv. Mater.* **2009**, *21*, 3191.
28. Sayil, C.; Okay, O. *Polym. Bull.* **2002**, *48*, 499.
29. Alzari, V.; Nuvoli, D.; Scognamillo, S.; Piccinini, M.; Gioffredi, E.; Malucelli, G.; Marceddu, S.; Sechi, M.; Sanna, V.; Mariani, A. *J. Mater. Chem.* **2011**, *21*, 8727.
30. Li, Z. Q.; Shen, J. F.; Ma, H. W.; Lu, X.; Shi, M.; Li, N.; Ye, M. X. *Soft Matter* **2012**, *8*, 3139.
31. Li, Z.; Shen, J.; Ma, H.; Lu, X.; Shi, M.; Li, N.; Ye, M. *Polym. Bull.* **2012**, *68*, 1153.
32. Li, Z.; Shen, J.; Ma, H.; Lu, X.; Shi, M.; Li, N.; Ye, M. *Mater. Sci. Eng. C* **2013**, *33*, 1951.
33. Han, D.; Yan, L. *ACS Sustain. Chem. Eng.* **2014**, *2*, 296.
34. Zhang, E.; Wang, T.; Lian, C.; Sun, W.; Liu, X.; Tong, Z. *Carbon* **2013**, *62*, 117.
35. Hummers, W. S.; Offeman, R. E. *J. Am. Chem. Soc.* **1958**, *80*, 1339.
36. Zhang, J.; Yang, H.; Shen, G.; Cheng, P.; Zhang, J.; Guo, S. *Chem. Commun.* **2010**, *46*, 1112.
37. Chen, T. Y.; Cao, Z.; Guo, X. L.; Nie, J. J.; Xu, J. T.; Fan, Z. Q.; Du, B. Y. *Polymer* **2011**, *52*, 172.
38. Otake, K.; Inomata, H.; Konno, M.; Saito, S. *Macromolecules* **1990**, *23*, 283.
39. Zhang, X.; Yang, Y.; Chung, T. *Langmuir* **2002**, *18*, 2538.
40. Schmaljohann, D. *Adv. Drug Deliv. Rev.* **2006**, *58*, 1655.
41. Yoshida, R.; Sakai, K.; Okano, T.; Sakurai, Y. *J. Biomater. Sci. Polym. Ed.* **1994**, *6*, 585.
42. Bae, Y. H.; Okano, T.; Kim, S. W. *Pharm. Res.* **1991**, *8*, 531.
43. Hou, Y.; Matthews, A. R.; Smitherman, A. M.; Bulick, A. S.; Hahn, M. S.; Hou, H.; Han, A.; Grunlan, M. A. *Biomaterials* **2008**, *29*, 3175.
44. Geever, L. M.; Devine, D. M.; Nugent, M. J. D.; Kennedy, J. E.; Lyons, J. G.; Hanley, A.; Higginbotham, C. L. *Eur. Polym. J.* **2006**, *42*, 2540.
45. Pan, Y.; Bao, H.; Sahoo, N. G.; Wu, T.; Li, L. *Adv. Funct. Mater.* **2011**, *21*, 2754.
46. Liu, J.; Yang, W.; Tao, L.; Li, D.; Boyer, C.; Davis, T. P. *J. Polym. Sci. Part A: Polym. Chem.* **2010**, *48*, 425.
47. Lo, C.; Zhu, D.; Jiang, H. *Soft Matter* **2011**, *7*, 5604.
48. Jin, S.; Bian, F.; Liu, M.; Chen, S.; Liu, H. *Polym. Int.* **2009**, *58*, 142.
49. Liu, J.; Chen, G.; Jiang, M. *Macromolecules* **2011**, *44*, 7682.
50. Fei, X.; Xu, S.; Feng, S.; Lin, J.; Lin, J.; Shi, X.; Wang, J. *J. Polym. Res.* **2011**, *18*, 1131.
51. Liu, F.; Urban, M. W. *Prog. Polym. Sci.* **2010**, *35*, 3.
52. Bhumkar, D. R.; Pokharkar, V. B. *AAPS PharmSciTech* **2006**, *7*, E50.
53. Gan, T.; Guan, Y.; Zhang, Y. *J. Mater. Chem.* **2010**, *20*, 5937.